



# Analysis of anomalous quartic $WWZ\gamma$ couplings in $\gamma p$ collision at the LHC



A. Senol<sup>a,\*</sup>, M. Köksal<sup>b</sup>

<sup>a</sup> Department of Physics, Abant İzzet Baysal University, 14280, Bolu, Turkey

<sup>b</sup> Department of Physics, Cumhuriyet University, 58140, Sivas, Turkey

## ARTICLE INFO

### Article history:

Received 2 December 2014

Received in revised form 7 January 2015

Accepted 19 January 2015

Available online 22 January 2015

Editor: A. Ringwald

## ABSTRACT

Gauge boson self-couplings are exactly determined by the non-Abelian gauge nature of the Standard Model (SM), thus precision measurements of these couplings at the LHC provide an important opportunity to test the gauge structure of the SM and the spontaneous symmetry breaking mechanism. It is a common way to examine the physics of anomalous quartic gauge boson couplings via effective Lagrangian method. In this work, we investigate the potential of the process  $pp \rightarrow p\gamma p \rightarrow pWZqX$  to analyze anomalous quartic  $WWZ\gamma$  couplings by two different, CP-violating and CP-conserving, effective Lagrangians at the LHC. We calculate 95% confidence level limits on the anomalous coupling parameters with various values of the integrated luminosity. Our numerical results show that the best limits obtained on the anomalous couplings  $\frac{k_0^W}{\Lambda^2}$ ,  $\frac{k_1^W}{\Lambda^2}$ ,  $\frac{k_2^W}{\Lambda^2}$  and  $\frac{a_n}{\Lambda^2}$  at  $\sqrt{s} = 14$  TeV and an integrated luminosity of  $L_{int} = 100 \text{ fb}^{-1}$  are  $[-1.37; 1.37] \times 10^{-6} \text{ GeV}^{-2}$ ,  $[-1.88; 1.88] \times 10^{-6} \text{ GeV}^{-2}$ ,  $[-6.55; 6.55] \times 10^{-7} \text{ GeV}^{-2}$  and  $[-2.21; 2.21] \times 10^{-6} \text{ GeV}^{-2}$ , respectively. Thus,  $\gamma p$  mode of photon-induced reactions at the LHC highly improves the sensitivity limits of the anomalous coupling parameters  $\frac{k_0^W}{\Lambda^2}$ ,  $\frac{k_1^W}{\Lambda^2}$ ,  $\frac{k_2^W}{\Lambda^2}$  and  $\frac{a_n}{\Lambda^2}$ .

© 2015 The Authors. Published by Elsevier B.V. This is an open access article under the CC BY license (<http://creativecommons.org/licenses/by/4.0/>). Funded by SCOAP<sup>3</sup>.

## 1. Introduction

The SM has been tested with many important experiments and it has been demonstrated to be quite successful, particularly after the discovery of a particle consistent with the Higgs boson with a mass of about 125 GeV [1,2]. Nevertheless, some of the most fundamental questions still remain unanswered. Especially, the strong CP problem, neutrino oscillations and matter–antimatter asymmetry have not been adequately clarified by the SM. It is expected to find answers to these problems of new physics beyond the SM. One of the ways of investigating new physics is to examine anomalous gauge boson interactions determined by non-Abelian  $SU_L(2) \times U_Y(1)$  gauge symmetry. Therefore, research on these couplings with a high precision can either confirm the gauge symmetry of the SM or give some hint for new physics beyond the SM. Any deviation of quartic couplings of the gauge bosons from the expected values would imply the existence of new physics beyond the SM. It is mostly common to examine new physics in a model

independent way via the effective Lagrangian method. This method is expressed by high-dimensional operators which lead to anomalous quartic gauge couplings. These high-dimensional operators do not generate new trilinear vertices. Thus, genuine quartic gauge couplings can be independently investigated from new trilinear gauge couplings.

In the literature, the anomalous quartic gauge boson couplings are commonly examined by two different CP-conserving and CP-violating effective Lagrangians. The first one, CP-violating effective Lagrangian is defined by [3]

$$L_n = \frac{i\pi\alpha}{4\Lambda^2} a_n \epsilon_{ijk} W_{\mu\alpha}^{(i)} W_\nu^{(j)} W^{(k)\alpha} F^{\mu\nu} \quad (1)$$

where  $F^{\mu\nu}$  is the electromagnetic field strength tensor,  $\alpha$  is the electroweak coupling constant,  $a_n$  is the strength of the parametrized anomalous quartic coupling and  $\Lambda$  stands for new physics scale. The anomalous  $WWZ\gamma$  vertex function generated by above effective Lagrangian is given in Appendix A.

Second, the CP-conserving effective operators can be written by using the formalism of Ref. [4]. There are fourteen effective photonic operators with respect to the anomalous quartic gauge couplings, and they are defined by 14 independent couplings  $k_{0,c}^{w,b,m}$ ,  $k_{1,2,3}^{w,m}$  and  $k_{1,2}^b$  which are all zero in the SM. These operators can

\* Corresponding author.

E-mail addresses: [senol\\_a@ibu.edu.tr](mailto:senol_a@ibu.edu.tr) (A. Senol), [mkoksal@cumhuriyet.edu.tr](mailto:mkoksal@cumhuriyet.edu.tr) (M. Köksal).

be expressed in terms of independent Lorentz structures. For example, there are four Lorentz invariant structures for the lowest dimension  $WW\gamma\gamma$  and  $ZZ\gamma\gamma$  interactions

$$W_0^\gamma = \frac{-e^2 g^2}{2} F_{\mu\nu} F^{\mu\nu} W^{+\alpha} W_\alpha^-, \quad (2)$$

$$W_c^\gamma = \frac{-e^2 g^2}{4} F_{\mu\nu} F^{\mu\alpha} (W^{+\nu} W_\alpha^- + W^{-\nu} W_\alpha^+), \quad (3)$$

$$Z_0^\gamma = \frac{-e^2 g^2}{4 \cos^2 \theta_W} F_{\mu\nu} F^{\mu\nu} Z^\alpha Z_\alpha, \quad (4)$$

$$Z_c^\gamma = \frac{-e^2 g^2}{4 \cos^2 \theta_W} F_{\mu\nu} F^{\mu\alpha} Z^\nu Z_\alpha. \quad (5)$$

Also, the two independent operators for the  $ZZ\gamma\gamma$  interactions are parameterized as the following

$$Z_0^Z = \frac{-e^2 g^2}{2 \cos^2 \theta_W} F_{\mu\nu} Z^{\mu\nu} Z^\alpha Z_\alpha, \quad (6)$$

$$Z_c^Z = \frac{-e^2 g^2}{2 \cos^2 \theta_W} F_{\mu\nu} Z^{\mu\alpha} Z^\nu Z_\alpha. \quad (7)$$

The five Lorentz structure belonging to  $WWZ\gamma$  interactions are given by

$$W_0^Z = -e^2 g^2 F_{\mu\nu} Z^{\mu\nu} W^{+\alpha} W_\alpha^-, \quad (8)$$

$$W_c^Z = -\frac{e^2 g^2}{2} F_{\mu\nu} Z^{\mu\alpha} (W^{+\nu} W_\alpha^- + W^{-\nu} W_\alpha^+), \quad (9)$$

$$W_1^Z = -\frac{e g_z g^2}{2} F^{\mu\nu} (W_{\mu\nu}^+ W_\alpha^- Z^\alpha + W_{\mu\nu}^- W_\alpha^+ Z^\alpha), \quad (10)$$

$$W_2^Z = -\frac{e g_z g^2}{2} F^{\mu\nu} (W_{\mu\alpha}^+ W^{-\alpha} Z_\nu + W_{\mu\alpha}^- W^{+\alpha} Z_\nu), \quad (11)$$

$$W_3^Z = -\frac{e g_z g^2}{2} F^{\mu\nu} (W_{\mu\alpha}^+ W_\nu^- Z^\alpha + W_{\mu\alpha}^- W_\nu^+ Z^\alpha) \quad (12)$$

with  $g = e/\sin\theta_W$ ,  $g_z = e/\sin\theta_W \cos\theta_W$  and  $V_{\mu\nu} = \partial_\mu V_\nu - \partial_\nu V_\mu$  where  $V = W^\pm, Z$ . Here, the CP-conserving anomalous  $WWZ\gamma$  vertex functions generated from Eqs. (8)–(12) are given in Appendix A.

Consequently, these fourteen effective photonic quartic operators can be simply expressed by

$$L = \frac{k_0^\gamma}{\Lambda^2} (Z_0^\gamma + W_0^\gamma) + \frac{k_c^\gamma}{\Lambda^2} (Z_c^\gamma + W_c^\gamma) + \frac{k_1^\gamma}{\Lambda^2} Z_0^\gamma + \frac{k_{23}^\gamma}{\Lambda^2} Z_c^\gamma + \frac{k_0^Z}{\Lambda^2} Z_0^Z + \frac{k_c^Z}{\Lambda^2} Z_c^Z + \sum_{i=0,c,1,2,3} \frac{k_i^W}{\Lambda^2} W_i^Z, \quad (13)$$

where

$$k_j^\gamma = k_j^w + k_j^b + k_j^m \quad (j = 0, c, 1), \quad (14)$$

$$k_{23}^\gamma = k_2^w + k_2^b + k_2^m + k_3^w + k_3^m, \quad (15)$$

$$k_0^Z = \frac{\cos\theta_W}{\sin\theta_W} (k_0^w + k_1^w) - \frac{\sin\theta_W}{\cos\theta_W} (k_0^b + k_1^b) + \left( \frac{\cos^2\theta_W - \sin^2\theta_W}{2 \cos\theta_W \sin\theta_W} \right) (k_0^m + k_1^m), \quad (16)$$

$$k_c^Z = \frac{\cos\theta_W}{\sin\theta_W} (k_c^w + k_2^w + k_3^w) - \frac{\sin\theta_W}{\cos\theta_W} (k_c^b + k_2^b) + \left( \frac{\cos^2\theta_W - \sin^2\theta_W}{2 \cos\theta_W \sin\theta_W} \right) (k_c^m + k_2^m + k_3^m), \quad (17)$$

$$k_0^W = \frac{\cos\theta_W}{\sin\theta_W} k_0^w - \frac{\sin\theta_W}{\cos\theta_W} k_0^b + \left( \frac{\cos^2\theta_W - \sin^2\theta_W}{2 \cos\theta_W \sin\theta_W} \right) k_0^m, \quad (18)$$

$$k_c^W = \frac{\cos\theta_W}{\sin\theta_W} k_c^w - \frac{\sin\theta_W}{\cos\theta_W} k_c^b + \left( \frac{\cos^2\theta_W - \sin^2\theta_W}{2 \cos\theta_W \sin\theta_W} \right) k_c^m, \quad (19)$$

$$k_j^W = k_j^w + \frac{1}{2} k_j^m \quad (j = 1, 2, 3). \quad (20)$$

For this study, we only take care of the  $k_i^W$  parameters (see Eqs. (18)–(20)) corresponding to the anomalous  $WWZ\gamma$  couplings. These  $k_i^W$  parameters are correlated with couplings defining anomalous  $WW\gamma\gamma$ ,  $ZZ\gamma\gamma$  and  $ZZZ\gamma$  interactions [4]. Hence, we require to distinguish the anomalous  $WWZ\gamma$  couplings from the other anomalous quartic couplings. This can be accomplished to apply extra restrictions on  $k_i^W$  parameters as suggested by Ref. [5]. The anomalous  $WWZ\gamma$  couplings can be only leaved by taking  $k_2^m = -k_3^m$  while the remaining parameters are equal to zero. As a result, we express the effective interaction of  $WWZ\gamma$  as follows

$$L_{\text{eff}} = \frac{k_2^m}{2\Lambda^2} (W_2^Z - W_3^Z). \quad (21)$$

Refs. [4–6] are phenomenologically investigated the  $\frac{k_2^m}{\Lambda^2}$  couplings defined the anomalous quartic  $WWZ\gamma$  vertex. In addition, the  $\frac{k_0^W}{\Lambda^2}$  and  $\frac{k_c^W}{\Lambda^2}$  couplings given in Eqs. (18)–(20) constitute the present experimental limits on the anomalous quartic  $WWZ\gamma$  couplings within CP-conserving effective Lagrangians. Therefore, in this study, we examine limits on the CP-conserving parameters  $\frac{k_0^W}{\Lambda^2}$ ,  $\frac{k_c^W}{\Lambda^2}$ ,  $\frac{k_2^m}{\Lambda^2}$  and the CP-violating parameter  $\frac{a_n}{\Lambda^2}$  to compare with the previous experimental and phenomenological results on the anomalous quartic  $WWZ\gamma$  gauge couplings in the literature.

The anomalous quartic  $WWZ\gamma$  couplings have been constrained by analyzing the processes  $e^+e^- \rightarrow W^+W^-Z$ ,  $W^+W^-\gamma$ ,  $W^+W^-(\gamma) \rightarrow 4f\gamma$  [8–12],  $e\gamma \rightarrow W^+W^-e$ ,  $\nu_e W^-Z$  [3,13] and  $\gamma\gamma \rightarrow W^+W^-Z$  [14,15] at linear  $e^+e^-$  colliders and its operating modes of  $e\gamma$  and  $\gamma\gamma$ . In addition, the potential of the process  $e^+e^- \rightarrow e^+\gamma^*e^- \rightarrow e^+W^-Z\nu_e$  [16] by making use of Equivalent Photon Approximation (EPA) at the CLIC to probe the anomalous quartic  $WWZ\gamma$  gauge couplings is examined. Finally, a detailed analysis of anomalous  $WWZ\gamma$  couplings at the LHC have been analyzed through the processes  $pp \rightarrow W(\rightarrow jj)\gamma Z(\rightarrow \ell^+\ell^-)$  [4] and  $W(\rightarrow \ell\nu_\ell)\gamma Z(\rightarrow \ell^+\ell^-)$  [6]. Up to now, in these studies, even though the anomalous quartic  $WWZ\gamma$  couplings are investigated via either CP-violating or CP-conserving effective Lagrangians, they are examined by using both effective Lagrangians solely by Refs. [6,16].

The LEP provides current experimental limits on  $a_n/\Lambda^2$  parameter of the anomalous quartic  $WWZ\gamma$  couplings determined by CP-violating effective Lagrangian. Recent limits obtained through the process  $e^+e^- \rightarrow W^+W^-\gamma$  by L3, OPAL and DELPHI Collaborations are

$$-0.14 \text{ GeV}^{-2} < \frac{a_n}{\Lambda^2} < 0.13 \text{ GeV}^{-2}, \quad (22)$$

$$-0.16 \text{ GeV}^{-2} < \frac{a_n}{\Lambda^2} < 0.15 \text{ GeV}^{-2}, \quad (23)$$

$$-0.18 \text{ GeV}^{-2} < \frac{a_n}{\Lambda^2} < 0.14 \text{ GeV}^{-2} \quad (24)$$

at 95% confidence level, respectively [17–19]. Nevertheless, the most stringent limits on  $k_0^W/\Lambda^2$  and  $k_c^W/\Lambda^2$  parameters described by CP-conserving effective Lagrangian are provided through the process  $q\bar{q}' \rightarrow W(\rightarrow \ell\nu)Z(\rightarrow jj)\gamma$  with an integrated luminosity

of  $19.3 \text{ fb}^{-1}$  at  $\sqrt{s} = 8 \text{ TeV}$  by CMS Collaboration at the LHC [7]. These are

$$-1.2 \times 10^{-5} \text{ GeV}^{-2} < \frac{k_0^W}{\Lambda^2} < 1 \times 10^{-5} \text{ GeV}^{-2} \quad (25)$$

and

$$-1.8 \times 10^{-5} \text{ GeV}^{-2} < \frac{k_c^W}{\Lambda^2} < 1.7 \times 10^{-5} \text{ GeV}^{-2}. \quad (26)$$

In the coming years, since the LHC will be upgraded to center-of-mass energy of 14 TeV, it is anticipated to introduce more restrictive limits on anomalous quartic gauge boson couplings.

Photon-induced processes were comprehensively examined in  $ep$  and  $e^+e^-$  collisions at the HERA and LEP, respectively. In addition to  $pp$  collisions at the LHC, photon-induced processes, namely  $\gamma\gamma$  and  $\gamma p$ , enable us to test of the physics within and beyond the SM. These processes occurring at centre-of-mass energies well beyond the electroweak scale are examined in an exactly undiscovered regime of the LHC. Although  $pp$  processes at the LHC reach very high effective luminosity, they do not a clean environment due to the remnants of both proton beams after the collision. On the other hand, since  $\gamma\gamma$  and  $\gamma p$  processes have better known initial conditions and much simpler final states, these interactions can compensate the advantages of  $pp$  processes. Initial state photons in  $\gamma\gamma$  and  $\gamma p$  processes can be described in the framework of the EPA [20]. In the EPA, while  $\gamma\gamma$  collisions are generated by two almost real photons emitted from protons,  $\gamma p$  collisions are produced by one almost real photon emitted from one incoming proton which then subsequently collides with the other proton. The emitted photons in these collisions have a low virtuality. Therefore, when a proton emits an almost real photon, it does not dissociate into partons. Almost real photons are scattered at very small angles from the beam pipe, and they carry a small transverse momentum. Furthermore, if the proton emits a photon, it scatters with a large pseudorapidity and cannot be detected from the central detectors. Hence, detection of intact protons requires forward detector equipment in addition to central detectors with large pseudorapidity providing some information on the scattered proton energy. For this purpose, ATLAS and CMS Collaborations have a program of forward physics with extra detectors located at 220 m and 420 m away from the interaction point which can detect the particles with large pseudorapidity [21,22]. Forward detectors can detect intact scattered protons with  $9.5 < \eta < 13$  in a continuous range of  $\xi$  where  $\xi$  is the proton momentum fraction loss described by  $\xi = (|\vec{p}| - |\vec{p}'|)/|\vec{p}|$ ;  $\vec{p}$  and  $\vec{p}'$  are the momentum of incoming proton and the momentum of intact proton, respectively. The relation between the transverse momentum and pseudorapidity of intact proton is as follows

$$p_T = \frac{\sqrt{E_p^2(1 - \xi)^2 - m_p^2}}{\cosh \eta} \quad (27)$$

where  $m_p$  is the mass of proton and  $E_p$  is the energy of proton.

$\gamma\gamma$  collisions are usually electromagnetic in nature and these reactions have less backgrounds compared to  $\gamma p$  collisions. On the other hand,  $\gamma p$  collisions can reach much higher energy and effective luminosity with respect to  $\gamma\gamma$  collisions [23,24]. These properties of  $\gamma p$  process might be significant in the investigation of new physics due to the high energy dependence of the cross section containing anomalous couplings. Most of the SM operators are of dimension four since only operators with even dimension satisfy conservation of lepton and baryon number. Therefore, the operators examining anomalous gauge boson self-couplings have to be

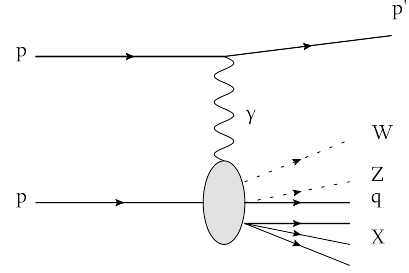


Fig. 1. Schematic diagram for the process  $pp \rightarrow p\gamma p \rightarrow pWZqX$ .

at least dimension six operators. For example, anomalous  $WWZ\gamma$  couplings are defined by dimension six effective Lagrangians, and have very strong energy dependences. Hence anomalous cross section including the  $WWZ\gamma$  vertex has a higher momentum dependence than the SM cross section. Therefore,  $\gamma p$  processes are anticipated to have a high sensitivity to anomalous  $WWZ\gamma$  couplings since it has a higher energy reach with respect to  $\gamma\gamma$  processes.

Photon-induced reactions were observed experimentally through the processes  $p\bar{p} \rightarrow p\gamma\gamma\bar{p} \rightarrow pe^+e^-\bar{p}$  [25,26],  $p\bar{p} \rightarrow p\gamma\gamma\bar{p} \rightarrow p\mu^+\mu^-\bar{p}$  [27],  $p\bar{p} \rightarrow p\gamma\bar{p} \rightarrow pWW\bar{p}$  [28] and  $p\bar{p} \rightarrow p\gamma\bar{p} \rightarrow pJ/\psi(\psi(2S))\bar{p}$  [29] by the CDF and D0 Collaborations at the Fermilab Tevatron. However, after these processes were examined at the Tevatron, this phenomenon has led to the investigation of potential of the LHC as a  $\gamma\gamma$  and  $\gamma p$  colliders for new physics researches. Therefore, photon-photon processes such as  $pp \rightarrow p\gamma\gamma p \rightarrow pe^+e^-p$ ,  $pp \rightarrow p\gamma\gamma p \rightarrow p\mu^+\mu^-p$ , and  $pp \rightarrow p\gamma\gamma p \rightarrow pW^+W^-p$  have been analyzed from the early LHC data at  $\sqrt{s} = 7 \text{ TeV}$  by the CMS Collaboration [30–32]. In addition, many studies on new physics beyond the SM through photon-induced reactions at the LHC in the literature have been phenomenologically examined. These studies contain: gauge boson self-interactions, excited neutrino, extradimensions, unparticle physics, and so forth [33–58]. In this work, we have examined the CP-conserving and CP-violating anomalous quartic  $WWZ\gamma$  couplings through the process  $pp \rightarrow p\gamma p \rightarrow pWZq'X$  at the LHC.

## 2. The cross sections and numerical analysis

An almost real photon emitted from one proton beam can interact with the other proton and generate  $W$  and  $Z$  bosons via deep inelastic scattering in the main process  $pp \rightarrow p\gamma p \rightarrow pWZq'X$ . A schematic diagram defining this main process is shown in Fig. 1. The reaction  $\gamma q \rightarrow WZq'$  participates as a subprocess in the main process  $pp \rightarrow p\gamma p \rightarrow pWZq'X$  where  $q = d, s, \bar{u}, \bar{c}$  and  $q' = u, c, d, \bar{s}$ . Corresponding tree level Feynman diagrams of the subprocess are shown in Fig. 2. As seen in Fig. 2, while only the first of these diagrams includes anomalous  $WWZ\gamma$  vertex, the others give SM contributions. We obtain the total cross section of  $pp \rightarrow p\gamma p \rightarrow pWZq'X$  process by integrating differential cross section of  $\gamma q \rightarrow WZq'$  subprocess over the parton distribution functions CTEQ6L [59] and photon spectrum in EPA by using the computer package CalcHEP [60].

In Figs. 3 and 4, we plot the integrated total cross section of the process  $pp \rightarrow p\gamma p \rightarrow pWZq'X$  as a function of the anomalous couplings. We collect all the contributions arising from subprocesses  $\gamma q \rightarrow WZq'$  while obtaining the total cross section. In addition, we presume that only one of the anomalous quartic gauge couplings is non-zero at any given time, while the other couplings are fixed to zero. We can see from Fig. 3 that deviation from SM value of the anomalous cross section containing the coupling  $\frac{k_0^W}{\Lambda^2}$  is larger than  $\frac{k_0^W}{\Lambda^2}$  and  $\frac{k_c^W}{\Lambda^2}$ . For this reason, the limits obtained on

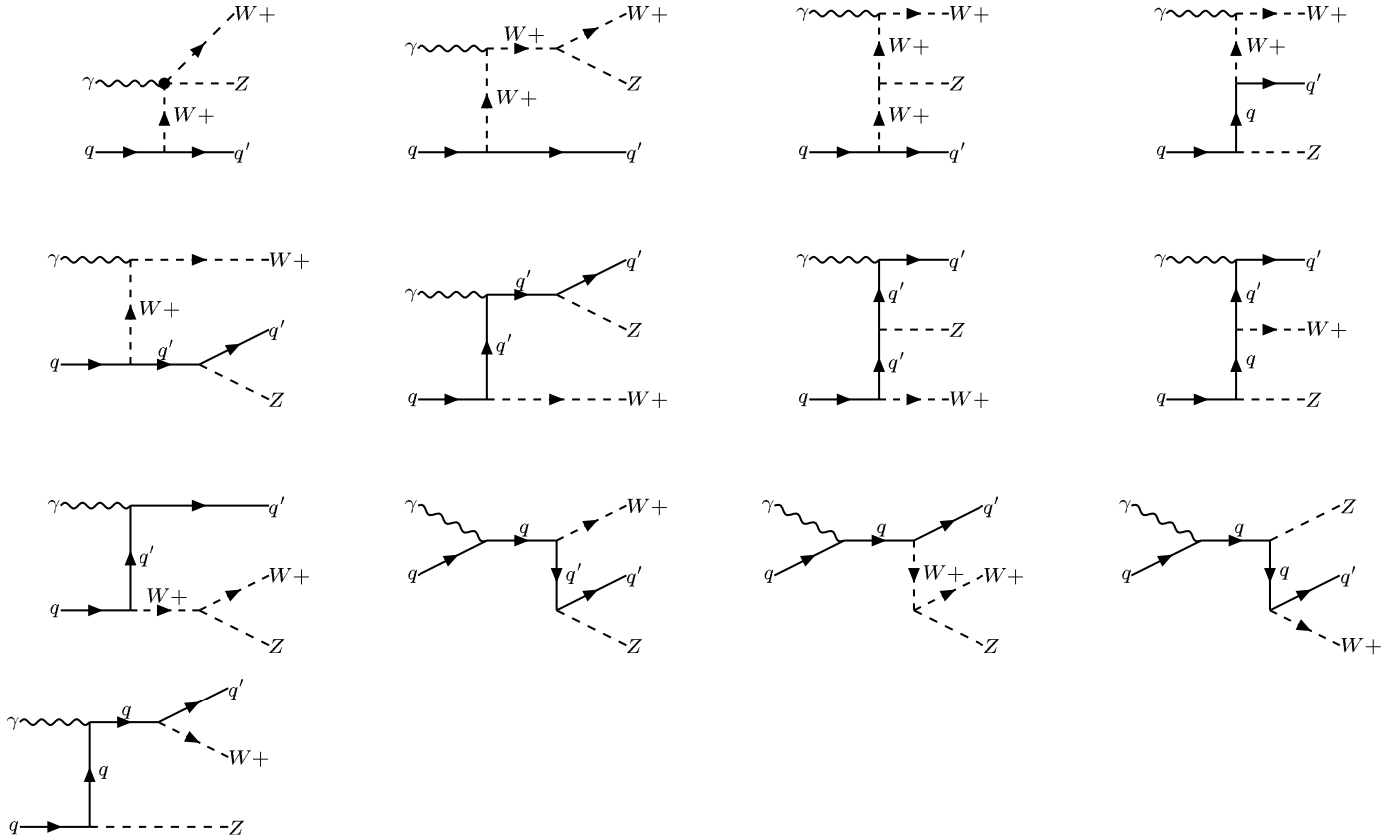


Fig. 2. Tree level Feynman diagrams for the subprocess  $\gamma q \rightarrow W Z q'$ .

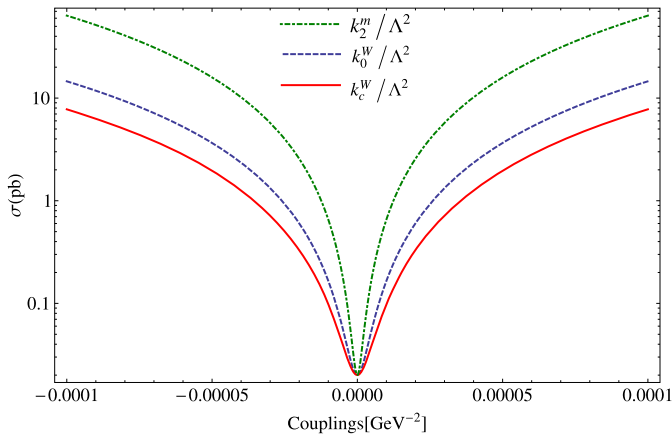


Fig. 3. The total cross sections as function of anomalous  $\frac{k_0^W}{\Lambda^2}$ ,  $\frac{k_c^W}{\Lambda^2}$  and  $\frac{k_2^m}{\Lambda^2}$  couplings for the process  $pp \rightarrow p\gamma p \rightarrow pWZqX$  at the LHC with  $\sqrt{s} = 14$  TeV.

the coupling  $\frac{k_2^m}{\Lambda^2}$  from analyzed process are anticipated to be more restrictive than the limits on  $\frac{k_0^W}{\Lambda^2}$  and  $\frac{k_c^W}{\Lambda^2}$ .

We calculate the sensitivity of the process  $pp \rightarrow p\gamma p \rightarrow pWZq'X$  to anomalous quartic gauge couplings by applying one and two-dimensional  $\chi^2$  criterion without a systematic error. The  $\chi^2$  function is defined as follows

$$\chi^2 = \left( \frac{\sigma_{SM} - \sigma_{NP}}{\sigma_{SM} \delta_{stat}} \right)^2 \quad (28)$$

where  $\sigma_{NP}$  is the cross section in the existence of new physics effects,  $\delta_{stat} = \frac{1}{\sqrt{N}}$  is the statistical error;  $N$  is the number of events.

The number of expected events of the process  $pp \rightarrow p\gamma p \rightarrow pWZq'X$  is obtained as the signal  $N = L_{int} \times \sigma_{SM} \times S \times BR(W \rightarrow \ell\nu_\ell) \times BR(Z \rightarrow q\bar{q}')$  where  $L_{int}$  denotes the integrated luminosity,  $\sigma_{SM}$  is the SM cross section and  $\ell = e^-$  or  $\mu^-$ . We consider strong interactions between the interacting protons. These interactions are generally performed by adding a correction factor to the integrated cross section, which is called the survival probability. Survival probability ( $S$ ) is described as the probability of the scattered protons not to dissociate due to the secondary interactions. This survival probability factor proposed for some photoproduction processes is  $S = 0.7$  [46,56,57]. The same survival factor is assumed for our process. We impose both cuts for transverse momentum of final state quarks to be  $p_T^j > 15$  GeV and the pseudorapidity of final state quarks to be  $|\eta| < 2.5$  since ATLAS and CMS have central detectors with a pseudorapidity coverage  $|\eta| < 2.5$ . The minimal transverse momentum cut of an outgoing proton is taken to be  $p_T > 0.1$  GeV within the photon spectrum. After applying these cuts, the SM background cross section for the process  $pp \rightarrow p\gamma p \rightarrow pWZqX$  at  $\sqrt{s} = 14$  TeV is obtained as 0.0201 pb.

For the processes with the high luminosity at the LHC, physics events called pile-up can give rise to an important background. However, in low luminosity values the pile-up of events is negligible in photoproduction interactions at the LHC. On the other hand, the LHC using some of the techniques (kinematics and timing constraints) can be operated at high luminosity such as  $100 \text{ fb}^{-1}$  as stated by Ref. [22].

In Tables 1–3, we give the one-dimensional limits on anomalous quartic gauge couplings  $\frac{k_0^W}{\Lambda^2}$ ,  $\frac{k_c^W}{\Lambda^2}$ ,  $\frac{k_2^m}{\Lambda^2}$  and  $\frac{a_n}{\Lambda^2}$  at 95% C.L. sensitivity at some integrated luminosities. Here, we consider that only one of the anomalous couplings changes at any time and center-of-mass energy of the  $pp$  system is taken to be  $\sqrt{s} = 14$  TeV. As

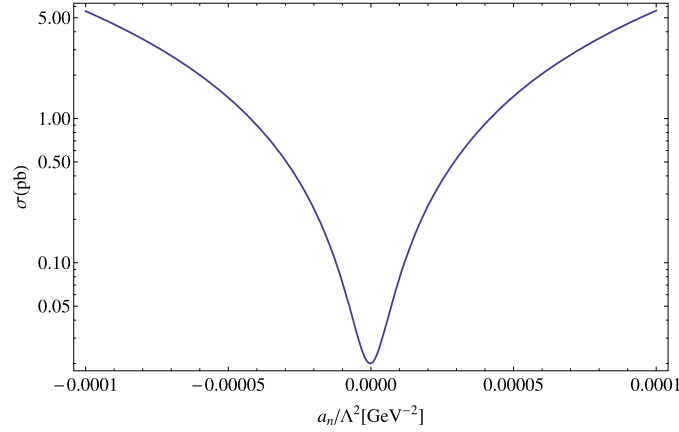


**Fig. 4.** The total cross section as function of anomalous  $\frac{a_n}{\Lambda^2}$  coupling for the process  $pp \rightarrow p\gamma p \rightarrow pWZqX$  at the LHC with  $\sqrt{s} = 14$  TeV.

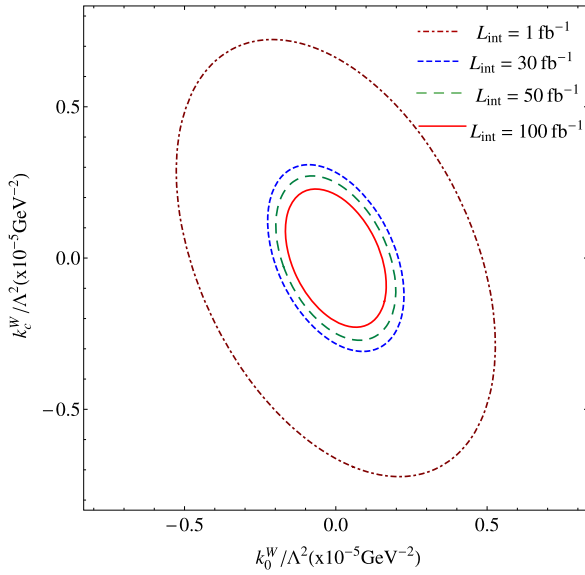


**Fig. 5.** 95% C.L. contours for anomalous  $\frac{k_0^W}{\Lambda^2}$  and  $\frac{k_c^W}{\Lambda^2}$  couplings for the process  $pp \rightarrow p\gamma p \rightarrow pWZqX$  at the LHC with  $\sqrt{s} = 14$  TeV.

**Table 1**

95% C.L. sensitivity limits of the anomalous  $\frac{k_0^W}{\Lambda^2}$  and  $\frac{k_c^W}{\Lambda^2}$  couplings through the process  $pp \rightarrow p\gamma p \rightarrow pWZqX$ . Here, center-of-mass energy of the  $pp$  system is taken to be  $\sqrt{s} = 14$  TeV.

$L_{int}$ (fb $^{-1}$ )	$\frac{k_0^W}{\Lambda^2}$ (GeV $^{-2}$ )	$\frac{k_c^W}{\Lambda^2}$ (GeV $^{-2}$ )
1	$[-4.33; 4.33] \times 10^{-6}$	$[-5.93; 5.93] \times 10^{-6}$
30	$[-1.85; 1.85] \times 10^{-6}$	$[-2.53; 2.53] \times 10^{-6}$
50	$[-1.63; 1.63] \times 10^{-6}$	$[-2.23; 2.23] \times 10^{-6}$
100	$[-1.37; 1.37] \times 10^{-6}$	$[-1.88; 1.88] \times 10^{-6}$

**Table 2**

95% C.L. sensitivity limits of the anomalous  $\frac{k_2^m}{\Lambda^2}$  couplings through the process  $pp \rightarrow p\gamma p \rightarrow pWZqX$ . Here, center-of-mass energy of the  $pp$  system is taken to be  $\sqrt{s} = 14$  TeV.

$L_{int}$ (fb $^{-1}$ )	$\frac{k_2^m}{\Lambda^2}$ (GeV $^{-2}$ )
1	$[-2.07; 2.07] \times 10^{-6}$
30	$[-8.85; 8.85] \times 10^{-7}$
50	$[-7.79; 7.79] \times 10^{-7}$
100	$[-6.55; 6.55] \times 10^{-7}$

can be seen from tables, our limits obtained on the couplings  $\frac{k_0^W}{\Lambda^2}$ ,  $\frac{k_c^W}{\Lambda^2}$  and  $\frac{a_n}{\Lambda^2}$  are at the order of  $10^{-6}$  GeV $^{-2}$  while limits on  $\frac{k_2^m}{\Lambda^2}$

**Table 3**

95% C.L. sensitivity limits of the anomalous  $\frac{a_n}{\Lambda^2}$  couplings through the process  $pp \rightarrow p\gamma p \rightarrow pWZqX$ . Here, center-of-mass energy of the  $pp$  system is taken to be  $\sqrt{s} = 14$  TeV.

$L_{int}$ (fb $^{-1}$ )	$\frac{a_n}{\Lambda^2}$ (GeV $^{-2}$ )
1	$[-7.00; 7.00] \times 10^{-6}$
30	$[-2.99; 2.99] \times 10^{-6}$
50	$[-2.63; 2.63] \times 10^{-6}$
100	$[-2.21; 2.21] \times 10^{-6}$

are at the order of  $10^{-7}$  GeV $^{-2}$ . In addition, it can be understood that limits on the coupling  $\frac{k_2^m}{\Lambda^2}$  are more restrictive than the limits on the couplings  $\frac{k_0^W}{\Lambda^2}$  and  $\frac{k_c^W}{\Lambda^2}$ . The sensitivities of the anomalous couplings in  $\frac{k_0^W}{\Lambda^2} - \frac{k_c^W}{\Lambda^2}$  plane at  $\sqrt{s} = 14$  TeV for various integrated luminosities are shown in Fig. 5. As we can see from Fig. 5, the best limits on anomalous couplings  $\frac{k_0^W}{\Lambda^2}$  and  $\frac{k_c^W}{\Lambda^2}$  at  $L_{int} = 100$  fb $^{-1}$  and  $\sqrt{s} = 14$  TeV are obtained as  $[-1.66; 1.66] \times 10^{-6}$  GeV $^{-2}$  and  $[-2.88; 1.88] \times 10^{-6}$  GeV $^{-2}$ , respectively.

The topology of photon-induced interactions can separately take place in diffractive processes. Diffractive processes are characterized by the exchange of a colorless composite object called as the pomeron. One of interactions including pomeron exchanges is single diffraction interaction. Therefore, we can consider single diffraction processes as a background of the analyzed process. A pomeron emitted by any of the incoming proton immediately after it collides with the other proton's quarks and this can produce same final state particles. In deep inelastic scattering process the virtuality of the struck quark is quite high. In our study, we take the virtuality of the struck quark  $Q^2 = m_Z^2$  where  $m_Z$  represents the  $Z$  boson's mass. For this reason, when a pomeron collides with a quark it may be dissociate into partons. These interactions generally culminate in higher multiplicities of final state particle due to existence of pomeron remnants [23]. Hence, pomeron remnants can be determined by the calorimeters and this background can be removed. In addition, the survival probability for a pomeron exchange is quite smaller than the survival probability of induced photons [24]. Hence, even though the background arising from pomeron-induced process are not annihilated, it cannot be too large with respect to the SM background contributions coming than the photon-induced process. It can be supposed that even if the background contribution of pomeron-induced process to our analyzed process is up to the SM background, all our limits with a 100 fb $^{-1}$  of integrated luminosity at  $\sqrt{s} = 14$  TeV are broken up to 3 times.

### 3. Conclusions

The LHC with forward detector equipment is a suitable platform to examine physics within and beyond the SM via  $\gamma\gamma$  and  $\gamma p$  processes.  $\gamma p$  process has the high luminosities and high center-of-mass energies compared to  $\gamma\gamma$  process. Moreover,  $\gamma p$  process due to the remnants of only one of the proton beams provides rather clean experimental conditions according to pure deep inelastic scattering of  $pp$  process. For these reasons, we examine the process  $pp \rightarrow p\gamma p \rightarrow pWZqX$  in order to determine anomalous quartic  $WWZ\gamma$  parameters  $\frac{k_0^W}{\Lambda^2}$ ,  $\frac{k_c^W}{\Lambda^2}$ ,  $\frac{k_2^m}{\Lambda^2}$  and  $\frac{a_n}{\Lambda^2}$  obtained by using two different CP-violating and CP-conserving effective Lagrangians at the LHC. A featured advantage of the process  $pp \rightarrow p\gamma p \rightarrow pWZqX$  is that it isolates anomalous  $WWZ\gamma$  couplings. It enables us to probe  $WWZ\gamma$  couplings independent of  $WW\gamma\gamma$ . Our limits on  $\frac{k_0^W}{\Lambda^2}$  and  $\frac{k_c^W}{\Lambda^2}$  are approximately one order better than the LHC's limits [7] while the limits obtained on  $\frac{a_n}{\Lambda^2}$  can set more stringent limit by five orders of magnitude compared to LEP results [17]. Moreover, we compare our limits with phenomenological studies on the anomalous  $\frac{k_2^m}{\Lambda^2}$  and  $\frac{a_n}{\Lambda^2}$  couplings at the LHC and CLIC. Ref. [16] have considered semi-leptonic decay channel of the final  $W$  and  $Z$  bosons in the cross section calculations to improve the limits on anomalous  $\frac{a_n}{\Lambda^2}$  and  $\frac{k_2^m}{\Lambda^2}$  couplings at the CLIC. We can see that the limits on anomalous  $\frac{a_n}{\Lambda^2}$  and  $\frac{k_2^m}{\Lambda^2}$  couplings expected to be obtained with  $L_{int} = 590 \text{ fb}^{-1}$  and  $\sqrt{s} = 3 \text{ TeV}$  are almost 3 times better than our best limits. Nevertheless, the limits on  $\frac{a_n}{\Lambda^2}$  by Ref. [6] have derived through  $W$  and  $Z$ 's pure leptonic decays at the LHC 14 TeV with  $100 \text{ fb}^{-1}$ . Our best limit is 10 times more restrictive than the best limit obtained in Ref. [6].

### Appendix A. The anomalous vertex functions for $WWZ\gamma$

The anomalous vertex for  $W^+(p_1^\alpha)W^-(p_2^\beta)Z(k_2^\nu)\gamma(k_1^\mu)$  with the help of effective Lagrangian (1) is generated as follows

$$i \frac{\pi\alpha}{4 \cos\theta_W \Lambda^2} a_n [g_{\alpha\nu} [g_{\beta\mu} k_1 \cdot (k_2 - p_1) - k_{1\beta} \cdot (k_2 - p_1)_\mu] - g_{\beta\nu} [g_{\alpha\mu} k_1 \cdot (k_2 - p_2) - k_{1\alpha} \cdot (k_2 - p_2)_\mu] + g_{\alpha\beta} [g_{\nu\mu} k_1 \cdot (p_1 - p_2) - k_{1\nu} \cdot (p_1 - p_2)_\mu] - k_{2\alpha} (g_{\beta\mu} k_{1\nu} - g_{\nu\mu} k_{1\beta}) + k_{2\beta} (g_{\alpha\mu} k_{1\nu} - g_{\nu\mu} k_{1\alpha}) - p_{2\nu} (g_{\alpha\mu} k_{1\beta} - g_{\beta\mu} k_{1\alpha}) + p_{1\nu} (g_{\beta\mu} k_{1\alpha} - g_{\alpha\mu} k_{1\beta}) + p_{1\beta} (g_{\nu\mu} k_{1\alpha} - g_{\alpha\mu} k_{1\nu}) + p_{2\alpha} (g_{\nu\mu} k_{1\beta} - g_{\beta\mu} k_{1\nu})]. \quad (\text{A.1})$$

In addition, the vertex functions for  $W^+(p_1^\alpha)W^-(p_2^\beta)Z(k_2^\nu)\gamma(k_1^\mu)$  produced from the effective Lagrangians (8)–(12) are expressed below

$$2ie^2 g^2 g_{\alpha\beta} [g_{\mu\nu} (k_1 \cdot k_2) - k_{1\nu} k_{2\mu}], \quad (\text{A.2})$$

$$i \frac{e^2 g^2}{2} [(g_{\mu\alpha} g_{\nu\beta} + g_{\nu\alpha} g_{\mu\beta}) (k_1 \cdot k_2) + g_{\mu\nu} (k_{2\beta} k_{1\alpha} + k_{1\beta} k_{2\alpha}) - k_{2\mu} k_{1\alpha} g_{\nu\beta} - k_{2\beta} k_{1\nu} g_{\mu\alpha} - k_{2\alpha} k_{1\nu} g_{\mu\beta} - k_{2\mu} k_{1\beta} g_{\nu\alpha}], \quad (\text{A.3})$$

$$ie g_z g^2 ((g_{\mu\alpha} k_1 \cdot p_1 - p_{1\mu} k_{1\alpha}) g_{\nu\beta} + (g_{\mu\beta} k_1 \cdot p_2 - p_{2\mu} k_{1\beta}) g_{\nu\alpha}) \quad (\text{A.4})$$

$$i \frac{e g_z g^2}{2} ((k_1 \cdot p_1 + k_1 \cdot p_2) g_{\mu\nu} g_{\alpha\beta} - (k_{1\alpha} p_{1\beta} + k_{1\beta} p_{2\alpha}) g_{\mu\nu} - (p_{1\mu} + p_{2\mu}) k_{1\nu} g_{\alpha\beta} + (p_{1\beta} g_{\mu\alpha} + p_{2\alpha} g_{\mu\beta}) k_{1\nu}), \quad (\text{A.5})$$

$$i \frac{e g_z g^2}{2} (k_1 \cdot p_1 g_{\mu\beta} g_{\nu\alpha} + k_1 \cdot p_2 g_{\mu\alpha} g_{\nu\beta} + (p_{1\nu} - p_{2\nu}) k_{1\beta} g_{\mu\alpha} - (p_{1\nu} - p_{2\nu}) k_{1\alpha} g_{\mu\beta} - p_{1\mu} k_{1\beta} g_{\nu\alpha} - p_{2\mu} k_{1\alpha} g_{\nu\beta}). \quad (\text{A.6})$$

### References

- [1] S. Chatrchyan, et al., CMS Collaboration, Phys. Lett. B 716 (2012) 30.
- [2] G. Aad, et al., ATLAS Collaboration, Phys. Lett. B 716 (2012) 1.
- [3] O.J.P. Eboli, M.C. Gonzalez-Garcia, S.F. Novaes, Nucl. Phys. B 411 (1994) 381.
- [4] O.J.P. Eboli, M.C. Gonzalez-Garcia, S.M. Lietti, Phys. Rev. D 69 (2004) 095005.
- [5] G. Belanger, F. Boudjema, Y. Kurihara, D. Perret-Gallix, A. Semenov, Eur. Phys. J. C 13 (2000) 283–293.
- [6] Ke Ye, Daneng Yang, Qiang Li, Phys. Rev. D 88 (1) (2013) 015023.
- [7] S. Chatrchyan, et al., CMS Collaboration, arXiv:1404.4619 [hep-ex].
- [8] G. Abu Leil, W.J. Stirling, J. Phys. G 21 (1995) 517.
- [9] W.J. Stirling, A. Werthenbach, Eur. Phys. J. C 14 (2000) 103.
- [10] A. Denner, et al., Eur. Phys. J. C 20 (2001) 201.
- [11] G. Montagna, et al., Phys. Lett. B 515 (2001) 197.
- [12] M. Beyer, et al., Eur. Phys. J. C 48 (2006) 353.
- [13] I. Sahin, J. Phys. G, Nucl. Part. Phys. 35 (2008) 035006.
- [14] O.J.P. Eboli, M.B. Magro, P.G. Mercadante, S.F. Novaes, Phys. Rev. D 52 (1995) 15.
- [15] I. Sahin, J. Phys. G, Nucl. Part. Phys. 36 (2009) 075007.
- [16] M. Köksal, A. Senol, arXiv:1406.2496.
- [17] P. Achard, et al., L3 Collaboration, Phys. Lett. B 527 (2002) 29.
- [18] J. Abdallah, et al., DELPHI Collaboration, Eur. Phys. J. C 31 (2003) 139.
- [19] G. Abbiendi, et al., OPAL Collaboration, Phys. Lett. B 580 (2004) 17.
- [20] V.M. Budnev, I.F. Ginzburg, G.V. Meledin, V.G. Serbo, Phys. Rep. 15 (1974) 181.
- [21] C. Royon, et al., RP220 Collaboration, in: Proceedings for the DIS 2007 Workshop, Munich, 2007, arXiv:0706.1796 [physics.ins-det].
- [22] M.G. Albrow, et al., FP420 R&D Collaboration, J. Instrum. 4 (2009) T10001.
- [23] J. de Favereau de Jeneret, V. Lemaître, Y. Liu, S. Olyn, T. Pierzchala, K. Piotrkowski, X. Rouby, N. Schul, M. Vander Donckt, arXiv:0908.2020 [hep-ph].
- [24] X. Rouby, Ph.D. thesis, Université Catholique de Louvain, 2008, UCL-Thesis 135-2008, CMS TS-2009/004.
- [25] A. Abulencia, et al., CDF Collaboration, Phys. Rev. Lett. 98 (2007) 112001.
- [26] T. Aaltonen, et al., CDF Collaboration, Phys. Rev. Lett. 102 (2009) 222002.
- [27] T. Aaltonen, et al., CDF Collaboration, Phys. Rev. Lett. 102 (2009) 242001.
- [28] V.M. Abazov, et al., D0 Collaboration, Phys. Rev. D 88 (2013) 012005.
- [29] T. Aaltonen, et al., CDF Collaboration, Phys. Rev. Lett. 102 (2009) 222002.
- [30] S. Chatrchyan, et al., CMS Collaboration, J. High Energy Phys. 1201 (2012) 052.
- [31] S. Chatrchyan, et al., CMS Collaboration, J. High Energy Phys. 1211 (2012) 080.
- [32] S. Chatrchyan, et al., CMS Collaboration, J. High Energy Phys. 1307 (2013) 116.
- [33] S. Atag, S.C. İnan, İ. Sahin, Phys. Rev. D 80 (2009) 075009.
- [34] İ. Şahin, et al., Phys. Rev. D 88 (2013) 095016.
- [35] S. Atag, S.C. İnan, İ. Sahin, J. High Energy Phys. 1009 (2010) 042.
- [36] A. Alboteanu, W. Kilian, J. Reuter, J. High Energy Phys. 0811 (2008) 010, arXiv:0806.4145 [hep-ph].
- [37] S.C. İnan, Phys. Rev. D 81 (2010) 115002.
- [38] S. Atag, A.A. Billur, J. High Energy Phys. 1011 (2010) 060.
- [39] İ. Sahin, A.A. Billur, Phys. Rev. D 83 (2011) 035011.
- [40] I. Sahin, Phys. Rev. D 85 (2012) 033002.
- [41] I. Sahin, M. Köksal, J. High Energy Phys. 1103 (2011) 100.
- [42] M. Köksal, S.C. İnan, Adv. High Energy Phys. 2014 (2014) 935840.
- [43] M. Köksal, S.C. İnan, Adv. High Energy Phys. 2014 (2014) 315826.
- [44] A.A. Billur, Europhys. Lett. 101 (2013) 21001.
- [45] B. Sahin, A.A. Billur, Phys. Rev. D 86 (2012) 074026.
- [46] A. Senol, Phys. Rev. D 87 (2013) 073003.
- [47] A. Senol, Int. J. Mod. Phys. A 29 (2014) 1450148, arXiv:1311.1370 [hep-ph].
- [48] A. Senol, A.T. Tasci, I.T. Cakir, O. Cakir, Mod. Phys. Lett. A 29 (2014) 1450186, arXiv:1405.6050 [hep-ph].
- [49] M. Tasevsky, Nucl. Phys. B, Proc. Suppl. 179–180 (2008) 187–195.
- [50] M. Tasevsky, arXiv:0910.5205.
- [51] H. Sun, Nucl. Phys. B 886 (2014) 691–711.
- [52] H. Sun, Chong-Xing Yue, Eur. Phys. J. C 74 (2014) 2823.
- [53] M. Tasevsky, Int. J. Mod. Phys. A 29 (2014) 1446012, arXiv:1407.8332 [hep-ph].
- [54] H. Sun, Phys. Rev. D 90 (2014) 035018, arXiv:1407.5356 [hep-ph].
- [55] I. Sahin, M. Köksal, S.C. İnan, A.A. Billur, B. Sahin, P. Tektas, E. Alici, R. Yildirim, arXiv:1409.1796 [hep-ph].
- [56] I. Sahin, B. Sahin, Phys. Rev. D 86 (2012) 115001.
- [57] V.A. Khoze, A.D. Martin, M.G. Ryskin, Eur. Phys. J. C 24 (2002) 459.
- [58] S. Fichet, G. von Gersdorff, J. High Energy Phys. 1403 (2014) 102, arXiv:1311.6815 [hep-ph].
- [59] J. Pumplin, D.R. Stump, J. Huston, H.L. Lai, P.M. Nadolsky, W.K. Tung, J. High Energy Phys. 0207 (2002) 012.
- [60] A. Belyaev, N.D. Christensen, A. Pukhov, Comput. Phys. Commun. 184 (2013) 1729, arXiv:1207.6082 [hep-ph].